# Frequency-domain meshless solver for acoustic wave equation using a stable radial basis-finite difference (RBF-FD) algorithm with hybrid kernels

*Pankaj K Mishra* and Sankar K Nath, Department of Geology and Geophysics, Indian Institute of Technology Kharagpur; Gregory E Fasshauer, Department of Applied Mathematics and Statistics, Colorado School of Mines; Mrinal K Sen, Institute for Geophysics, Jackson School of Geoscience, University of Texas at Austin.*

**Summary**

We present a stable meshless scheme for numerical solution of 2D Helmholtz equation using radial basis-finite difference (RBF-FD) method. The interpolants over a 'user defined' node arrangement are computed through a hybrid Gaussian-cubic kernel. Such a hybrid kernel reduces the ill-conditioning problem in the discretization, therefore, making it applicable to the problems with relatively larger degrees of freedom. Numerical tests demonstrate that the presented RBF-FD with the hybrid kernel has significant improvements over standard mesh-based finite difference as well as conventional RBF-FD approaches with either Gaussian or cubic kernel. We discuss the different node arrangements, the stability condition of the system matrix, convergence, and numerical dispersion, and finally use the presented RBF-FD algorithm for frequency-domain modeling of acoustic wave propagation in homogeneous as well as layered half-space. In order to suppress the spurious reflections from computational boundaries, absorbing boundary conditions has been effectively incorporated.

**Introduction**

Helmholtz solver is a widely used tool in computational geosciences due to its applications in many fields like multisource experiments (Pratt and Worthington, 1990), frequency-domain acoustic wave modeling (Dablain, 1986; Amini and Javaherian, 2011; Liu, 2014), frequency-domain elastic wave modeling (Li et al., 2015), seismic imaging (Plessix, 2006), and computational electromagnetics (Wannamaker et al., 1987, Singh and Sharma, 2015), etc. Frequency-domain modeling of wave propagation has certain advantages over time-domain modeling: (1) it provides a mutiscale approach in inversion by staging from the low to high frequencies, (2) it is relatively easy to incorporate attenuation in the model, and (3) frequency-domain full waveform inversion can manage and process relatively less volumes of seismic data by limiting the inversion to a limited number of frequency components (Sirgue and Pratt, 2004). The choice of an appropriate wave propagation solver, its grid-dispersion nature, and error convergence has been an active field of research in the past few decades.

The kernel-based finite difference approach is a relatively new meshless method for numerical solution of partial differential equations. Since radial basis functions (RBFs) are a popular choice as kernels in such a meshless method, it is frequently referred to as the RBF-FD approach. RBF-FD method was initially proposed by Tolstykh et al., (2003), where they used RBFs, in finite difference mode to solve PDEs. The approach has been consistently improved (Fornberg and Flyer, 2015) and applied to various problems in science and engineering including convention-diffusion (Chandhini and Sanyasiraju, 2007), atmospheric global electric circuit (Bayona et al., 2010), shallow water simulation (Flyer et al., 2012), reaction-diffusion on surfaces (Shankar et al., 2015), and time-domain elastic wave propagation in 2D isotropic media (Martin et al., 2015), etc.

The Gaussian kernel is known to provide exponential convergence in strong-form meshless methods; however, it limits their applications to a limited number of nodes in the domain as the resulting linear system becomes ill-conditioned, at large degrees of freedom (Mishra and Nath, 2016). To deal with such an ill-conditional problem with RBFs, Mishra et al., (2016) proposed a hybrid kernel by using a combination of Gaussian and a polyharmonic spline (PHS) kernel. Such a hybrid kernel was found to compute stable interpolants on scattered nodes for relatively large degrees of freedom and to reduce the ill-conditioning problem in radial basis-pseudospectral (RBF-PS) approach for numerical solution of PDEs (Mishra et al., 2017). Here, we use the hybrid Gaussian-cubic kernel in RBF-FD — a localized representation of RBF-PS to solve the frequency-domain acoustic wave equation coupled with absorbing boundary conditions. Figure 1 shows 2D visualization of a typical hybrid kernel against the conventional Gaussian kernel.

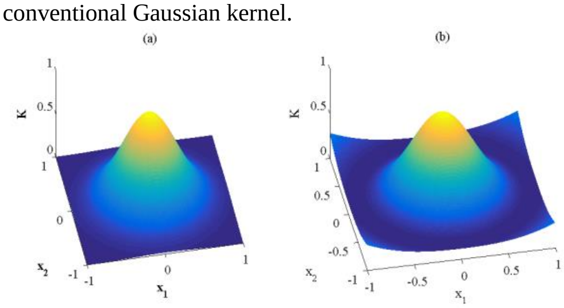


Figure 1: 2D visualization of the pure Gaussian (left) and the hybrid kernel with 10% cubic (right).

### Governing Equations

In the context of full waveform inversion and modeling the attenuation process, it is often required to solve the acoustic wave equation in frequency-domain, which is given by

$$\nabla^2 p(\mathbf{x},\omega) + \frac{\omega^2}{c(\mathbf{x})^2} p(\mathbf{x},\omega) = f(\mathbf{x},\omega). \qquad (1)$$

where $p(\mathbf{x},\omega)$ is the pressure wavefield, $f(\mathbf{x},\omega)$ is the energy source, $c(\mathbf{x})$ is the primary wave velocity and $\omega$ is the angular frequency.
In order to suppress the spurious reflections from the truncated computational boundary, we include absorbing boundary conditions as given by

$$\frac{\partial p(\mathbf{x},\omega)}{\partial \mathbf{n}} + i\frac{\omega}{c(\mathbf{x})} p(\mathbf{x},\omega) = 0. \qquad (5)$$

### RBF-FD Discretization

We explain the RBF-FD discretization approach with a general boundary value problem (Helmholtz type) in a general computational domain $\Omega$ as:

$$\mathbf{L}u(\mathbf{x}) = f(\mathbf{x}), \qquad (6)$$

where, $\mathbf{L}$ is a general linear differential operator ($\mathbf{L} = \nabla^2 + k^2$, for Helmholtz equation), $u(\mathbf{x})$ is a field, $f(x)$ is a source term and $\mathbf{x}$ represents the spatial coordinate. A general boundary condition for equation (6) can be written as:

$$\mathbf{B}u(\mathbf{x}) = g(\mathbf{x}). \qquad (7)$$

$\mathbf{B}$ is a general differential operator at the boundary. For Dirichlet boundary condition $\mathbf{B}=1$ and for Neumann boundary condition $\mathbf{B} = \partial/\partial n$; where $n$ is the unit outward normal. The first step in any meshless method is to create nodes inside the given computational domain. Figure 2(a-d) shows some typical node arrangements in a 2D domain. Next step is to define a scheme for selection of a finite number of neighbor points for each node. In order to compute a differentiation matrix at each point, only those neighboring points will be considered. There are several ways to select neighbor nodes; one of them is to select the neighbors falling within a user defined radius. Such an approach is frequently used in local meshless methods and more recently in RBF-FD too. This approach often requires some 'ghost nodes' outside the computational domain for computing the differentiation operator at the boundary points. However, in this work, we choose an alternate approach for choosing the neighbors. Instead of defining a distance based support domain, for each node, we define a finite number of closest points as neighbors. The advantage of this approach is that it does not require extension of the computational domain for approximation at the boundary points. A typical representation of such an approach has been shown in Figure 2e. As an approximation, an unknown field $u$ can be represented by using a kernel $\phi$ as:

$$\hat{u}(x) = \Phi(x)^T \mathbf{K}^{-1}\mathbf{u}, \qquad (8)$$

where $\mathbf{K}$ is the global RBF interpolation matrix. The basic assumption here is that since the kernel-based interpolation provided a good approximation ($\hat{u}$) of a field $u$, any operator applied on ($\hat{u}$) will be a reasonable approximation of the same operator applied on the true field (Fasshauer and McCourt, 2015). Therefore, we can write:

$$\mathbf{L}\hat{u}(x) = \mathbf{L}\Phi(x)^T \mathbf{K}^{-1}\mathbf{u}. \qquad (9)$$

If we performed such an approximation at the points $(x_1 ... x_N)$ and used the following notation:

$$\mathbf{K_L} = \begin{bmatrix} \mathbf{L}\Phi(x_1)^T \\ \vdots \\ \mathbf{L}\Phi(x_N)^T \end{bmatrix}, \qquad (10)$$

we can write the discretizion $\mathbf{L}$ (an $N \times N$ matrix) of the linear operator $\mathbf{L}$ as:

$$\mathbf{L} = \mathbf{K_L}\mathbf{K}^{-1}. \qquad (11)$$

At this stage, since the interpolation matrix is global, *i.e.*, all the points have been considered while computing the interpolation matrix, the discrete operator in equation (11) has a global nature. The idea for RBF-FD discretization is to consider only a 'few' neighbor points to compute the discrete operator at a location (kernel centers). In order to have a more specific discussion using the neighbor nodes, let us assume that we need to compute the RBF-FD derivative at locations $\chi = \{x_1, ..., x_N\}$. For the $i^{th}$ node $x_i$, consider the number of neighbor nodes equal to $n_{x_i}$. We will collect the stencils at locations $Z = \{\mathrm{z}_1, ... \mathrm{z}_N\}$. Therefore, the local differential operator at the stencil $\mathbf{x}_i$ can be written as:

$$\mathbf{L}_i = \mathbf{K}_{\mathbf{L}}^{x_i}\mathbf{K}_{z_i}^{-1}. \qquad (12)$$

In an RBF-FD discretization, we compute various local differentiation matrices ($\mathbf{L}_i$) and place them at specific locations in a global differentiation matrix $\mathbf{L}^{FD}$, as given by

$$\mathbf{L}^{FD}=\begin{bmatrix}\mathbf{K}_{\mathcal{L}}^{x_1}\mathbf{K}_{z_1}^{-1}P_1\\ \vdots \\ \mathbf{K}_{\mathcal{L}}^{x_N}\mathbf{K}_{z_N}^{-1}\,\mathrm{P}_N\end{bmatrix}, \qquad (13)$$

where $P_i \in \{0,1\}^{n_{x_i}\times N}$ is an incidence matrix which has been defined to place the nodes $z_i$ (at which $\mathbf{L}_i$ has been computed) to the correct position in the sparse row of $\mathbf{L}^{FD}$. The elements of $P_i$ are given by

$$[P_i]_{k,l}=\begin{cases}1 & if\ k=l,\\ 0 & else.\end{cases} \qquad (14)$$

Thus, the discrete representation of the problem defined by equations (6) and (7), can be written as

$$\begin{bmatrix}\mathbf{L}^{FD}\\ \mathbf{B}^{FD}\end{bmatrix}[\mathbf{c}]=\begin{bmatrix}f\\ g\end{bmatrix}, \qquad (15)$$

where $\mathbf{B}^{FD}$ is the discretized operator which needs to be applied at the boundary points, and calculated in a similar manner as $\mathbf{L}^{FD}$. Equation (15) has been written by assuming only Dirichlet boundary condition; however, different boundary conditions can be incorporated by creating the corresponding rows in it.

## Numerical Tests

We start with a simple test of solving the above frequency-domain problem in a domain $[0,1]\times[0,1]$ with a constant velocity $c=1$. The spatial domain is discretized using $50\times 50$ equally spaced Cartesian nodes. We incorporate the discrete Dirac-delta function as the seismic source, which is expressed as

$$f(x,z,\omega)=\frac{1}{(h_x h_z)}\delta(s_x)\delta(s_z) \quad . \qquad (16)$$

For a point source located at $(s_x,s_z)=(0.2,0.8)$ and grid interval as $h_x=h_z=0.02$. Figure 3 shows the approximate solution of this problem using RBF-FD and its comparison to the exact solution, which are in good agreement. We further solve the same problem in a larger domain $[0m,400m]\times[0m,400m]$. The goal of this numerical test is to demonstrate the efficacy of the solution for a practical range of frequencies, which are typically used for modeling acoustic wave propagation in exploration seismology. We consider a typical Ricker source, which in frequency domain, is represented as:

$$s(x,z,f)=\frac{2f^2}{\pi f_c^3}\exp\left(-\frac{f^2}{\pi f^2}\right)\delta(x_s)\delta(z_s) \quad , \qquad (17)$$

where $f=\omega/2\pi$, and $f_c=\overline{f}\left(3\sqrt{\pi}\right)$ is related to the cut off frequency $\overline{f}$ (Moreira et al., 2014). Figure 4 shows the real component of the frequency-domain approximated wavefield for low and high frequencies, which suggests that the approximated solution does not disperse at relatively high frequencies.

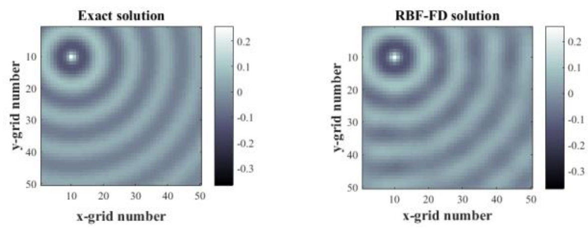


Figure 3: Exact versus RBF-FD solution comparison

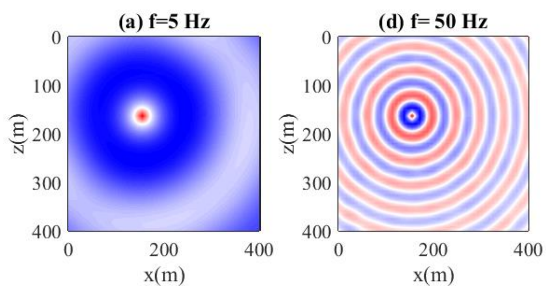


Figure 4: RBF-FD solution at low and high frequencies.

We further solve the acoustic forward problem in the frequency-domain for a set of frequencies and then transform the solution into the time domain by using the inverse Fourier transform. We compare the time-domain RBF-FD solution with that obtained by a 9-point mixed-grid finite difference method. We compute the FD solution by following the 9-point mixed grid formulation, and a different Ricker source used in (Amini and Javaherian, 2011), as shown in Figure 5. They are in good agreement.

## Conclusion

We have developed a stable meshfree wave propagation solver using RBF-FD with hybrid Gaussian-cubic kernel. The approach does not suffer from the 'pollution effect' due to grid-dispersion. Use of hybrid kernel allows the RBF-FD scheme to be applicable for relatively higher degrees of freedom compared to those obtained through pure Gaussian or cubic kernel.

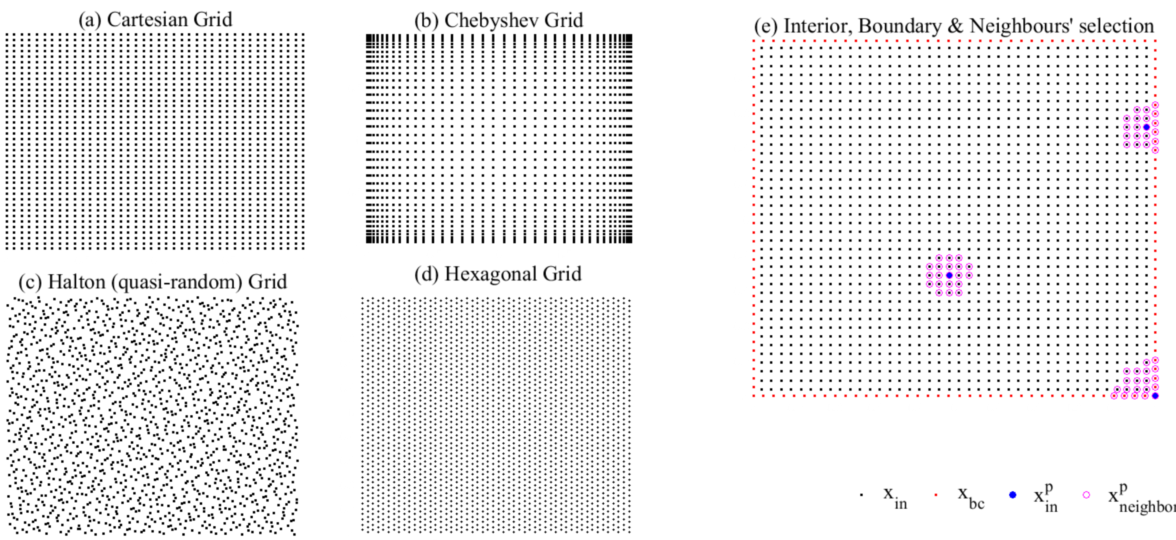


Figure 2: Testing the RBF-FD scheme for various node distributions including Cartesian, Chebyshev, quasi random and random nodes in terms of RMS error, sparsity patterns and eigenvalue stability. The abbreviations SPY and RCM stand for simple and RCM ordering

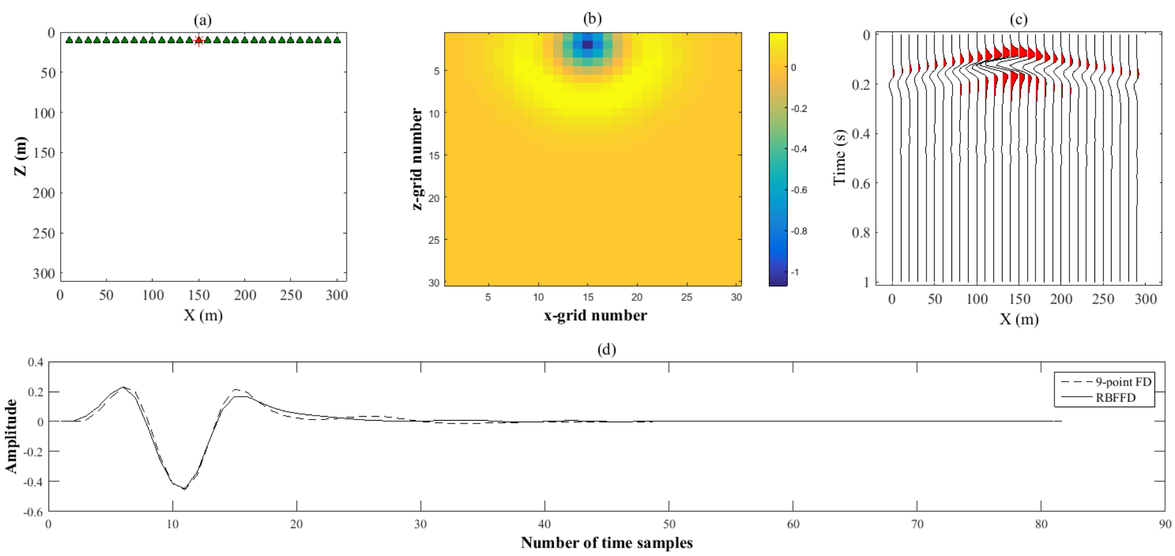


Figure 5: (a) The computational domain and the location of source and receivers, (b) acoustic wavefield at t = 0.1750s, (c) shot gather of seismograms, and (d) comparison of the seismogram passing through the source location, computed using RBF-FD and 9 point FD with 100m thick perfectly matched layer.

**EDITED REFERENCES**

Note: This reference list is a copyedited version of the reference list submitted by the author. Reference lists for the 2017 SEG Technical Program Expanded Abstracts have been copyedited so that references provided with the online metadata for each paper will achieve a high degree of linking to cited sources that appear on the Web.

**REFERENCES**

Amini, N., and A. Javaherian, 2011, AMATLAB-based frequency-domain finite-difference package for solving 2d visco-acoustic wave equation: Waves in Random and Complex Media, **21**, 161–183, http://doi.org/10.1080/17455030.2010.537708.

Bayona, V., M. Moscoso, M. Carretero, and M. Kindelan, 2010, RBF-FD formulas and convergence properties: Journal of Computational Physics, **229**, 8281–8295, https://doi.org/10.1016/j.jcp.2010.07.008.

Chandhini, G., and Y. V. S. S. Sanyasiraju, 2007, Local RBF-FD solutions for steady convection diffusion problems: International Journal for Numerical Methods in Engineering, **72**, 352–378, https://doi.org/10.1002/nme.2024.

Dablain, M. A., 1986, The application of high-order differencing to the scalar wave equation: Geophysics, **51**, 54–66, https://doi.org/10.1190/1.1442040.

Fasshauer, G. E., and M. McCourt, 2015, Kernel-based approximation methods using MATLAB: World Scientific.

Flyer, N., E. Lehto, S. Blaise, G. B. Wright, and A. St-Cyr, 2012, A guide to RBF-generated finite differences for nonlinear transport: Shallow water simulations on a sphere: Journal of Computational Physics, **231**, 4078–4095, https://doi.org/10.1016/j.jcp.2012.01.028.

Fornberg, B., and N. Flyer, 2015, Solving PDEs with radial basis functions: Acta Numerica, **24**, 215–258, https://doi.org/10.1017/S0962492914000130.

Liu, Y., 2014, An optimal 5-point scheme for frequency-domain scalar wave equation: Journal of Applied Geophysics, **108**, 19–24, https://doi.org/10.1016/j.jappgeo.2014.06.006.

Li, Y. Y., Z. C. Li, and K. Zhang, 2015, Frequency-domain elastic full-waveform multiscale inversion method based on dual-level parallelism: Applied Geophysics, **12**, 545–554, https://doi.org/10.1007/s11770-015-0519-8.

Martin, B., B. Fornberg, and A. St-Cyr, 2015, Seismic modeling with radial-basis-function generated finite differences: Geophysics, **80**, no. 4, T137–T146, https://doi.org/10.1190/geo2014-0492.1.

Mishra, P. K. and S. K. Nath, 2016, On the convergence of iterative methods and pseudoinverse approaches in global meshless collocation: International Journal of Applied and Computational Mathematics, 1–14, https://doi.org/10.1007/s40819-016-0272-6.

Mishra, P. K., S. K. Nath, M. K. Sen, and G. E. Fasshauer, 2016, Hybrid Gaussian-cubic radial basis functions for scattered data interpolation: http://arxiv.org/abs/1512.07584.

Mishra, P. K., S. K. Nath, G. Kosec, and M. K. Sen, 2017, An improved radial basis-pseudospectral scheme with hybrid Gaussian-cubic kernels: Engineering Analysis with Boundary Elements, **80**, 162–171, https://doi.org/10.1016/j.enganabound.2017.03.009.

Moreira, R. M., M. A. Cetale Santos, J. L. Martins, D. L. F. Silva, R. B. V. Pessolani, D. M. S. Filho, and A. Bulcão, 2014, Frequency-domain acoustic-wave modeling with hybrid absorbing boundary conditions: Geophysics, **79**, no. 5, A39–A44, https://doi.org/10.1190/geo2014-0085.1.

Plessix, R. E., 2007, A Helmholtz iterative solver for 3D seismic-imaging problems: Geophysics, **72**, no. 5, SM185–SM194, https://doi.org/10.1190/1.2738849.

Pratt, R. G., and M. H. Worthington, 1990, Inverse theory applied to multi-source crosshole tomography. Part 1: Acoustic wave-equation method: Geophysical Prospecting, **38**, 287–310, http://doi.org/10.1111/j.1365-2478.1990.tb01846.x.

Shankar, V., G. B. Wright, R. M. Kirby, and A. L. Fogelson, 2015, A radial basis function (RBF)-finite difference (FD) method for diffusion and reaction–diffusion equations on surfaces: Journal of Scientific Computing, **63**, 745–768, https://doi.org/10.1007/s10915-014-9914-1.

Singh, A. and S. P. Sharma, 2015, Fast imaging of subsurface conductors using very low-frequency electromagnetic data: Geophysical Prospecting, **63**, 1355–1370, https://doi.org/10.1111/1365-2478.12323.

Sirgue, L., and R. G. Gerhard, 2004, Efficient waveform inversion and imaging: A strategy for selecting temporal frequencies: Geophysics, **69**, 231–248, https://doi.org/10.1190/1.1649391.

Tolstykh, I. A., and A. D. Shirobokov, 2003, On using radial basis functions in a "finite difference mode" with applications to elasticity problems: Computational Mechanics, **33**, 68–79, https://doi.org/10.1007/s00466-003-0501-9.

Wannamaker, P. E., J. A. Stodt, and L. Rijo, 1987, A stable finite element solution for two-dimensional magnetotelluric modelling: Geophysical Journal of the Royal Astronomical Society, **88**, 277–296, https://doi.org/10.1111/j.1365-246X.1987.tb01380.x.